

Proceedings of the Korean Nuclear Autumn Meeting  
Yongpyong, Korea, October 2002

## Two-Phase Measurement with Electromagnetic Flowmeters in the Liquid Metal Two-Phase Flow and Water-Air Two-Phase Flow

JaeEun Cha, YehChan Ahn, KyungWoo Seo, KyoungBo Ko, and MooHwan Kim

Pohang University of Science and Technology  
San 31, Hyoja Dong,  
Pohang, Korea, 790-784

### **Abstract**

In order to investigate the characteristics of an electromagnetic flowmeter in the liquid metal two-phase flow, AC electromagnetic flowmeters were designed and manufactured. Two-phase flow experiments, encompassing bubbly to slug flow regimes, were conducted with the water-air mixture and the liquid sodium-nitrogen mixture, respectively. The simple relation  $\Delta U_{TP} = \Delta U_{SP}/(1-\alpha)$ , relating flowmeter signal between single-phase flow and two-phase flow, was verified with measurements of the potential difference and the void fraction( $\alpha$ ) for a bubbly flow regime. Whereas there is no difference in the shape of the raw signal between single-phase flow and bubbly flow, the signal amplitude of bubbly flow is greater than that of single-phase flow under the same water flow and liquid sodium flow rates, since the passage area of the liquid flow is reduced. In the case of slug flow, the phase and the amplitude of the flowmeter output show a dramatic change in the flow characteristics around each slug bubble and the position of a slug bubble itself. Therefore, the electromagnetic flowmeter shows a good potential as a useful device for identifying the flow regimes. The void fraction can be simply measured with two electromagnetic flowmeters for a low-void fraction flow such as bubbly flow with some error margins. Thus, the flowmeters can be used to measure the void fraction for a liquid sodium within some tolerable error margins.

### **1. Introduction**

The thermal and hydraulic characteristics related with sodium two-phase flow have been required to satisfy the design and operational standards for its safety and economic maintenance. In case of a liquid metal, the two-phase measurement is very difficult due to the plugging and contamination with oxidation, and the limit of the sensor endurance at high temperature. A visual investigation of flow pattern is impossible due to the inherent opacity.

The objective of this research is to investigate the characteristics of electromagnetic flowmeters in the liquid metal two-phase flow. Thus a general water-air two-phase loop was

previously constructed before the setup of the liquid metal loop since the hydraulic properties of liquid sodium are similar to those of water.

The test sections of both loops were made of 1 inch inner diameter. Since the signal output of AC electromagnetic flowmeter has the phase and amplitude information simultaneously, it is more convenient to amplify and to study the characteristics of two-phase flow. In the present study, AC electromagnetic flowmeters, which were operated with low frequency sinusoidal excitation, were prepared to measure the liquid metal two-phase flow and the water-air two-phase flow.

On the base of the water-air loop, a liquid sodium-nitrogen loop was designed and fabricated for the vertical upward concurrent two-phase flow. To verify the accuracy of flowmeters, a single-phase flow experiment was previously conducted. Thus the liquid metal two-phase flow was investigated with an AC electromagnetic flowmeter as a non-contact method from bubbly to slug flow regime. The test range of superficial liquid velocity for this study was from 0.09 to 0.4 m/s and Hartmann number for the AC electromagnetic flowmeter in the test-section was about 100 at 190 °C. The void fraction could be measured with two electromagnetic flowmetes and its value was compared with that of water-air results.

## 2. Historical Review and Basic Theory

Shercliff<sup>(1)</sup> derived the electromagnetic flowmeter theory for the flow measurement of liquid metal and developed the idea of a weight function. From this weighting function, he showed that for a flowmeter with a uniform magnetic field and point electrodes, any axisymmetric rectilinear flow profile with the average flow velocity  $v_m$  gives rise to the signal  $\Delta U = Bv_m d$ . Elrod and Fouse<sup>(2)</sup> derived a relation permitting the calculation of the induced emf in case of an axisymmetric flow bounded by a conducting wall and conducted experiments with mercury. Bernier and Brennen<sup>(3)</sup> investigated the use of electromagnetic flowmeter in the two-phase flow. They concluded that a homogenous two-phase flow would give rise to a potential difference  $\Delta U_{TP} = \Delta U_{SP} / (1 - \alpha)$ . Furthermore, they concluded that  $\Delta U_{TP} = \Delta U_{SP} / (1 - \alpha)$  was also valid irrespective of flow regimes or the homogeneity of electrical conductivity. Wyatt<sup>(4)</sup> argued that the above conclusions are correct when the disperse phase consists of uniformly-distributed, small, randomly-oriented particles, which creates a macroscopically uniform, isotropic suspension. Two-phase experiments with electromagnetic flowmeters were studied by Hori<sup>(5)</sup>, Ochiai<sup>(6)</sup>, and Murakami<sup>(7)</sup>.

Velt<sup>(8)</sup>, and Krafft<sup>(9)</sup> studied the use of transformer signal for the measurement of two-phase flow. Heineman<sup>(10)</sup> suggested a method to measure the void fraction with two electromagnetic flowmeters and performed experiments in the NaK-argon mixtures for the comparison with their theory and verified the values of void fraction with gamma-ray attenuation method.

Bevir<sup>(11)</sup> extended the weight function of Shercliff to a three-dimensional weight vector. The solution of the flowmeter equation is described by

$$\Delta U_{AB} = \iiint_{\tau} \mathbf{v} \cdot \mathbf{W} d\tau \quad (1)$$

where  $\mathbf{W}$  is called the weight vector and it weights the contribution to  $\Delta U$  due to the velocity  $\mathbf{v}$  at every point.  $\mathbf{W}$  is given by  $\mathbf{W} = \mathbf{B} \times \mathbf{j}$ . The integral is taken over the flowmeter volume  $\tau$ . The virtual current  $\mathbf{j}$  weights the effect at electrodes of elemental  $\mathbf{B} \times \mathbf{v}$  generators at every

point in the liquid. Wyatt<sup>(4)</sup> tried to simplify the Equation (1) when the flow is rectilinear and axisymmetric [ $\mathbf{v} = \mathbf{v}(0,0,v(r))$ ] and the transverse magnetic field is uniform [ $\mathbf{B} = \mathbf{B}(B,0,0)$ ] with point-electrode. Wyatt<sup>(4)</sup> obtained that the potential difference between electrodes is proportional to flowrate regardless of velocity profile (so called “axisymmetric property”) i.e.

$$\Delta U_{AB} = W' \int_0^b 2\pi v(r) r dr = \text{Const} \cdot Q. \quad (2)$$

where  $W'$  is the axisymmetric weight function. The proportional constant can be obtained for a special case of rectilinear axisymmetric conditions, i.e. rectilinear uniform velocity [ $\mathbf{v} = \mathbf{v}(0,0,v)$ ]. Thus

$$\Delta U_{AB} = \frac{2B}{\pi b} Q = 2Bvb \quad (3)$$

and it holds for all rectilinear axisymmetric flow and uniform transverse magnetic field if taking the mean velocity  $v_m$  instead of  $v$ . In the case of bubbly flow it may be considered as a uniform and isotropic suspension as before. Hence the signal can be expressed as Equation (4).

$$\Delta U_{TP} = \frac{2B}{\pi b} \frac{Q_L}{1-\alpha} = \frac{\Delta U_{SP}}{1-\alpha} \quad (4)$$

Here,  $Q_L$  is liquid flow rate and  $\Delta U_{TP}$  is the potential difference between electrodes for two-phase bubbly flow and  $\Delta U_{SP}$  for liquid flow only (at the same flow rate  $Q_L$ ).

Figure 1 shows the schematic diagram for void fraction measurement with electromagnetic flowmeters. The mass balance between the inlet before injection of gaseous phase and the test-position can be expressed as an Equation (5).

$$\begin{aligned} \dot{m}_{fo} + \dot{m}_{go} &= \dot{m}_{f1} + \dot{m}_{g1} \\ \dot{m}_{go} &= \rho_{go} A_{go} v_{go}, \quad \dot{m}_{g1} = \rho_{g1} A_{g1} v_{g1} \\ \dot{m}_{fo} &= \rho_{fo} A_{fo} v_{fo}, \quad \dot{m}_{f1} = \rho_{f1} A_{f1} v_{f1} \end{aligned} \quad (5)$$

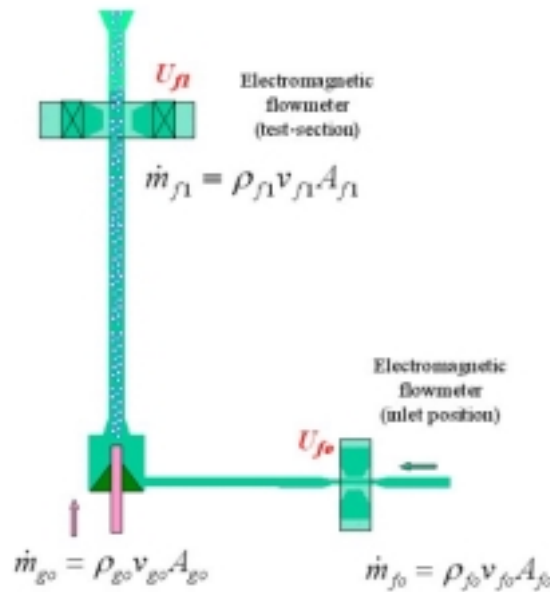


**Figure 1. Void-fraction measurement with em-flowmeters**

where  $\dot{m}$  is the mass flow rate of each fluid,  $\rho$  is the density,  $A$  is the cross-sectional area of flow tube, and  $v$  is the velocity. The subscripts  $g$  and  $f$  denote the gas-phase and liquid-phase, subscripts  $o$  and  $l$  means the inlet position before injection of gaseous phase and test-position respectively. From equation (5), the void fraction can be expressed with Equation (6).

$$\begin{aligned}\dot{m}_{fo} &= \dot{m}_{fl} \\ \rho_{fo}A_{fo}v_{fo} &= \rho_{fl}A_l(1-\alpha)v_{fl}, \quad U = KBvd \\ \alpha &= 1 - \left( \frac{\rho_{fo}}{\rho_{fl}} \right) \left( \frac{d_{fo}}{d_l} \right) \left( \frac{U_{fo}}{U_{fl}} \right) \left( \frac{B_l}{B_{fo}} \right) \left( \frac{K_l}{K_{fo}} \right)\end{aligned}\quad (6)$$

where  $U$  is the potential difference between electrodes,  $d$  is the distance between electrodes(inner diameter of flow tube), and  $K$  is the correction factor which is determined with flowmeter geometry and operating conditions. To calculate the void fraction  $\alpha$  with Equation (6), the correction factor  $K$  should be previously determined. The ratio of correction factor ( $K_l / K_{fo}$ ) can be expressed with Equation (7) for the electrically conducting wall under the uniform magnetic field, axisymmetric rectilinear flow, and negligible end-effect.

$$\frac{K_{fo}}{K_l} = \frac{1 + \left(\frac{d_l}{D_l}\right)^2 + \frac{\sigma_w}{\sigma_{TP}} \left[ 1 - \left(\frac{d_l}{D_l}\right)^2 \right]}{1 + \left(\frac{d_o}{D_o}\right)^2 + \frac{\sigma_w}{\sigma_o} \left[ 1 - \left(\frac{d_o}{D_o}\right)^2 \right]}\quad (7)$$

where  $\sigma_w$  is the conductivity of tube wall,  $\sigma_{TP}$  is the conductivity of two-phase flow, and  $D$  is the outer diameter of flowtube. The electrical conductivity  $\sigma_{TP}$  was calculated with experimental correlation suggested by Petrick<sup>(12)</sup> in Equation (8).

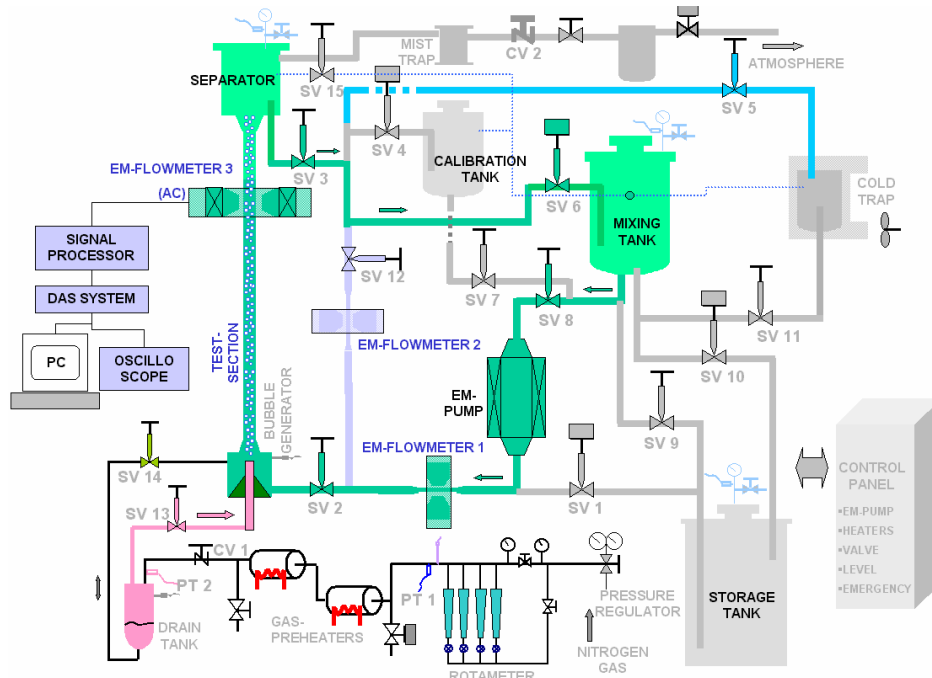
$$\sigma_{TP} = \frac{(1-\alpha)^2}{1+\alpha} \sigma_o, \quad 0 \leq \alpha \leq 0.70\quad (8)$$

### 3. Experimental Facilities and Methods

Figure 2 shows the schematic diagram of the experimental facility for the liquid metal two-phase flow. This facility was operated with a liquid sodium-nitrogen in a vertical test section for the concurrent two-phase flow. The vertical test-section was made by stainless steel pipe (25mm I.D. ~ 34mm O.D., SUS316) and an electromagnetic flowmeter in the test section was installed 60  $D_i$  (inner diameter of test-section) at a distance from the bubble generator. The loop is composed of the liquid-circulation loop and the gas-supply loop and the test-section for the mixing of two-phase. The liquid sodium in the mixing tank was pumped with an electromagnetic pump and was entered into the test-section through the em-flowmeter1 (master meter) and the bubble generator.

The electromagnetic flowmeter1 with permanent magnets was used as a master meter for the calibration of other flowmeters. The electromagnetic flowmeter3 was composed of an electromagnet, a pair of electrodes, and a flowtube. The electromagnet of the electromagnetic

flowmeter3 was sinusoidally excited by the AC power, which was controlled by a frequency converter (Fujitsu Denso M2PS1000) and an Uninterruptible Power System(UPS).



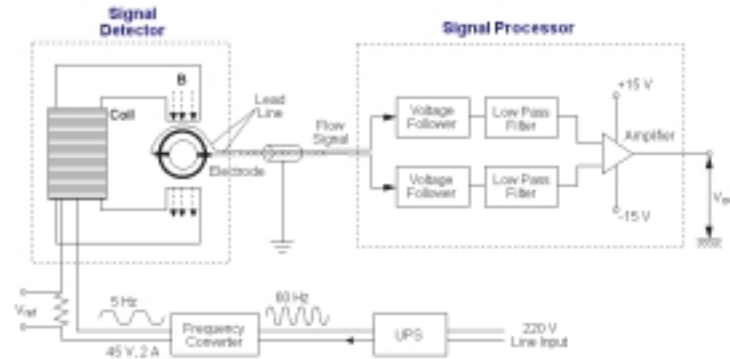
**Figure 2. Schematics of liquid Na-N<sub>2</sub> two-phase loop**

Figure 3 shows the schematic diagram of a signal processing unit. One of the greatest difficulties in electromagnetic flowmeter design is that the amplitude of the voltage across the electrodes is in the order of a few millivolts, which is relatively small when compared to extraneous voltages and noise. The main noise sources of the electromagnetic flowmeters, excited by AC power, are as follows:

- 1) Transformer signal by alternating magnetic field (including effect of the eddy current in the flowtube)
- 2) Noise by capacitive and resistive coupling between signal and power circuits

To avoid the difficulties stated above, a somewhat complex signal processing unit was needed. The signal processor has an input stage with voltage followers, a filtering stage and an amplifying stage with a gain of 400. To cancel out the differential noise(transformer signal), a counter differential noise was generated intentionally before voltage followers with a kind of pick-up coil(Watanabe<sup>(13)</sup>) and variable resistor. The reference resistor with 1  $\Omega$  and 10 W was used to get the reference voltage having the same phase as that of excitation current. From the reference voltage, the information about the characteristics of the magnetic field can be inferred, and the comparison between flow signal and noise is possible.

The mixing tank which was used to store and expand the liquid sodium during the test. The liquid sodium in the test-section was separated from the mixed phase at the separator and was returned into the mixing tank through the sodium valves SV3 and SV6.



**Figure 3. Schematic diagram of signal processing unit**

The nitrogen gas was upwardly injected into the test section through the orifice of the bubble generator by way of the sodium valve SV13. It was mixed with liquid sodium to make a two-phase flow. After separated, it was vented into the atmosphere through the mist trap and the check valve CV2. The flow rate of nitrogen gas was measured with four rotameters and controlled by the pressure regulator and several valves. Two sets of gas preheaters are mounted to reduce thermal non-equilibrium due to temperature difference between the liquid sodium and the nitrogen gas. The nitrogen gas was emitted through seven holes on gas-injector. The orifice holes in the bubble generator were uniformly disposed by considering the above estimation and the bubble formation with this orifice was visibly confirmed by the water-air experiment.

The flow rate of the liquid sodium was controlled with an electromagnetic pump and measured with electromagnetic flowmeters. The electromagnetic pump was designed and fabricated in the level of laboratory to drive the liquid sodium for this experiment. The power control of the pump was conducted with a variable AC power source (10 kVA-3 phase).

The calibration tank was installed to measure the volume of liquid sodium for the calibration of the electromagnetic flowmeters. A storage tank was used to store the solid sodium for the safety and was located the lowest part of the facility since the liquid sodium have to return by gravity in an emergency or after turning down of the system power. A total of 80 liter of solid sodium has been stored in the storage tank. The mist trap was mounted to remove the sodium vapor and particles in the nitrogen gas during the venting process. The cold trap was used to filter the impurities in the liquid sodium due to the contamination of the liquid metal with the precipitation method.

Most part of the piping system was made by stainless steel pipe with 1 inch inner diameter (SUS304, 1 inch schedule 40) and was connected with welding for the prevention of leakage of the sodium. The sodium valve SV1, SV6, SV7, and SV10 were automatically operated by the compressed air with 5 kgf/cm<sup>2</sup> gage pressure.

Every tank has independently heated with its heating system and the ceramic wool with 2 inch thickness was used for the thermal insulation. The temperature control of the piping system and test section were divided with seven parts for the effective heating and the ceramic wool of 1 inch thickness was used for thermal insulation. The liquid metal loop was usually charged with the cover gas (argon) to prevent oxidation of sodium. The control panel was used to control the preheaters of the piping system, the heaters of tanks, an electromagnetic pump, several automatic valves, and the cooling fan of the cold trap.

The electromagnetic flowmeter1 was calibrated as a master meter. The flowmeter signal and other data were acquired with the data acquisition board (Metabyte DAS-1802ST/DA). The calibration of the master meter was started with the opening and closing the sodium valves SV4 and SV6 simultaneously. The signal of the flowmeter was acquired with data acquisition board and the time required for the volume increment was measured with a stopwatch. The two-phase experiments were conducted in the test-section on the base of results of the master meter calibration.

#### 4. Experimental Results

The two-phase test was conducted in the range from bubbly to slug(Cha, Ahn, and Kim<sup>(14)</sup>). In case of water-air test, the void fraction was calculated by pressure-drop measurement between pressure-taps in the flange of magnetic flowmeter. The total pressure drop  $\Delta P$  between two-points in a vertical channel can be written as

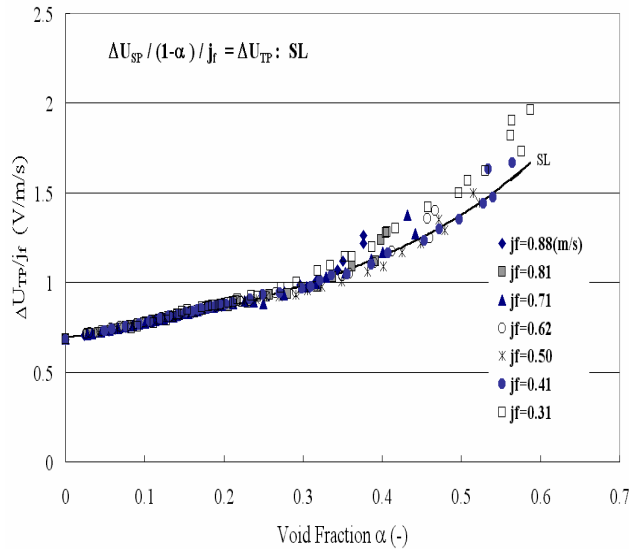
$$\Delta P = \Delta P_h + \Delta P_{tp} + \Delta P_{ac} \quad (9)$$

being given by the sum of the hydrostatic head  $\Delta P_h$ , the two-phase frictional pressure drop  $\Delta P_{tp}$ , and the accelerational pressure drop  $\Delta P_{ac}$ . The accelerational pressure drop can be neglected with respect to the hydrostatic head due to the no-phase change and the low superficial liquid velocity. The average void fraction was calculated by Equation (10) with the hydrostatic head (Lockhart<sup>(15)</sup>, Georges<sup>(16)</sup>)

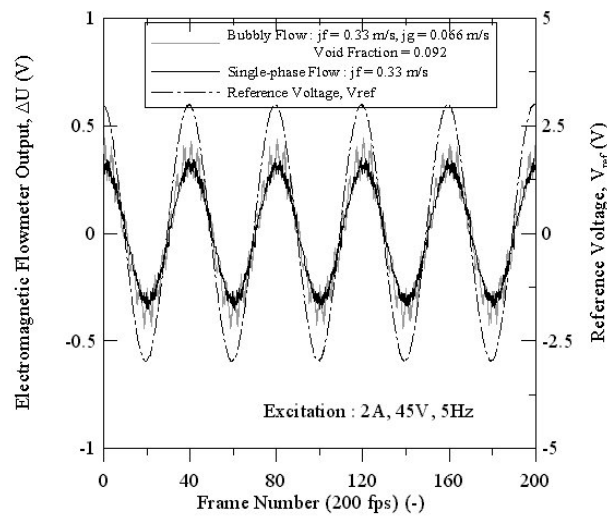
$$\alpha = 1 - \frac{\Delta P_h}{\rho_f g \Delta z} \quad (10)$$

Figure 4 was obtained by the normalization of output signal of electromagnetic flowmeter with superficial liquid velocity  $j_f$ . From this figure, the flowmeter output was linearly changed within bubbly flow region ( $\alpha < 0.3$ ) with void fraction and superficial liquid velocity  $j_f$ . The solid line plotted in this figure was obtained with the simple relation  $\Delta U_{TP} = \Delta U_{SP} / (1 - \alpha)$ , which  $\Delta U_{SP}$  obtained from the single-phase calibration data. The deviation of the measured data from the line calculated was considered that it was partially due to the measurement limitation of void fraction with pressure drop and partially inherent characteristics of electromagnetic flowmeter for the measurement of void fraction. In other words, it is understood from Figure 4 that the electromagnetic flowmeter can be used to measure the void fraction within low void fraction such as bubbly flow with a good performance and that the flow-pattern map made by Mishima and Ishii<sup>(17)</sup> was very good indicator for the criteria from bubbly to slug due to above reason.

Figure 5 shows the raw signal of the electromagnetic flowmeter in bubbly flow, the magnet being excited by an AC power source (2A, 5Hz). The reference voltage (dot-dash line) has the same phase as the magnetic flux  $\mathbf{B}$ , exciting current  $I_{ex}$ , and the flow signal  $V_m$ . The solid-line and dotted-line are output signals of the flowmeter in single-phase and bubbly flow, respectively. There is no difference between single-phase and bubbly flow in the shape of the raw signal. The signal amplitude of bubbly flow, however, is higher than single-phase even if we supply the same water flow rate  $Q_L$ . This results from the flow-passage reduction by void insertion in the flowtube.



**Figure 4. Normalized output of electromagnetic flowmeter with void fraction (water-air)**



**Figure 5. Raw signal of electromagnetic flowmeter in the bubbly flow (water-air)**

The raw signal of slug flow in Figure 6 is much more complicated than bubbly or single-phase flow. Therefore, it is necessary to acquire it with increased exciting frequency (20 Hz). The dot-dash line is the reference voltage, and the solid line is the output signal of the flowmeter. Matching the movement of a slug with the flowmeter output signal, a high speed CCD was used at a rate of 200 frames per second. Each case of Figure 6 corresponds to Figure 7. As a result of magnetic field  $\mathbf{M}$  perpendicular to transverse axis  $a-a'$ , eddy currents  $i_1$  and  $i_2$  are induced within the flow tube in the regions on either side of axis  $a-a'$ . When the magnetic fields and other conditions in the respective regions are perfectly symmetrical, then equal currents  $i_1$  and  $i_2$  of opposite polarity will flow and no resultant voltage will be

developed across the electrodes a and a' for a homogeneous flow in magnetic field zone. But when asymmetry exists, then a transformer signal would be produced which adversely affects the accuracy of the flow rate reading (Watanabe<sup>(13)</sup>).

Even though the flowmeter was tuned previously for removing the transformer emf and the leakage voltage, slug flow, unlike bubbly flow, breaks the tuning point since the symmetry of the upper and lower sides about the central electrode plane varies continuously. In other words, since the upper and lower eddy currents are not symmetric about the central electrode, the resultant of the transformer emf is mixed with motional emf ( $V_m$ ).

At point A (frame 30), there is no slug bubble in the test section and the upper and lower side are so symmetric with respect to electrode plane that the flowmeter output has motional emf only, and its phase is in phase with the reference voltage.

But at point B the phases are  $90^\circ$  different, where a slug occupies the lower half. In this case, the eddy current generated in the lower half has its minimum value and eddy current in

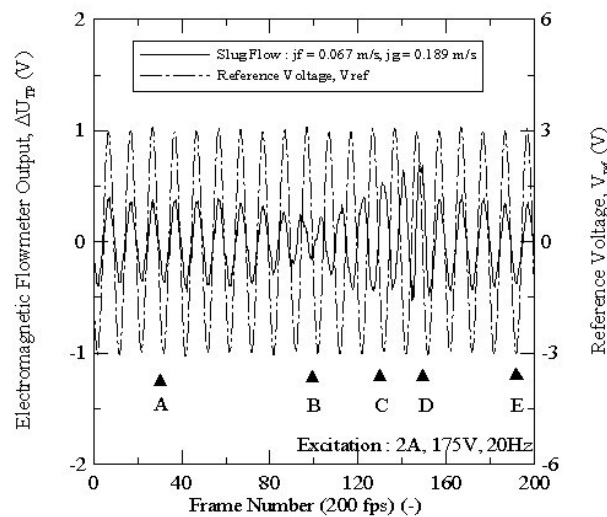


**Figure 6. Raw signal of electromagnetic flowmeter in the slug flow**

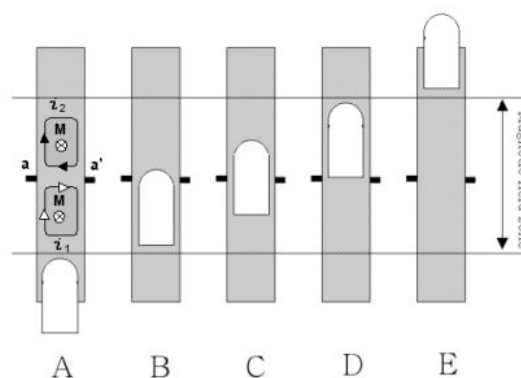


**Figure 7. Slug positions corresponding to indicators in Figure 6**

the upper half remains. Therefore, the resultant of the transformer emf by the imbalance of upper and lower eddy current has a maximum. On the other hand, the amplitude of the flowmeter output is reduced as approaching point B (frame 92). It represents the decreasing of the liquid mean velocity due to the following slug bubble.

At point C (frame 120), the phases are  $180^\circ$  different, showing that the transformer emf was not included at all, and the liquid mean velocity was inverted to a negative flow direction. From the high speed CCD, we determined that the slug was positioned in the midst of the test section. Around point C, the increasing amplitude of the flowmeter output shows that the inverted liquid mean velocity around the nose of the slug increases, until reaching a terminal velocity around the tail of the slug.

When reaching point D (frame 150), we can get the  $270^\circ$  out of phase situation due to the opposite action of eddy-currents compare with point B. Since the liquid mean velocity is abruptly dropped in the wake region of slug-bubble, the amplitude of flowmeter output is also steeply decreased. The slug configuration is opposite to that of point B.

Figure 8 shows the calibration chart of the DC electromagnetic flowmeters made in this study, under the condition of single-phase flow (liquid sodium at  $190^\circ\text{C}$ ). The output signal of these flowmeters for the mean velocity was calibrated using the volume measurement with a calibration tank in the LM (Liquid Metal) loop.

Figure 9 shows the single-phase calibration data of AC electromagnetic flowmeter which was excited with frequency converter (5Hz-2.5A-30V). Since there were various noises, the difference was existed nearby zero velocity.

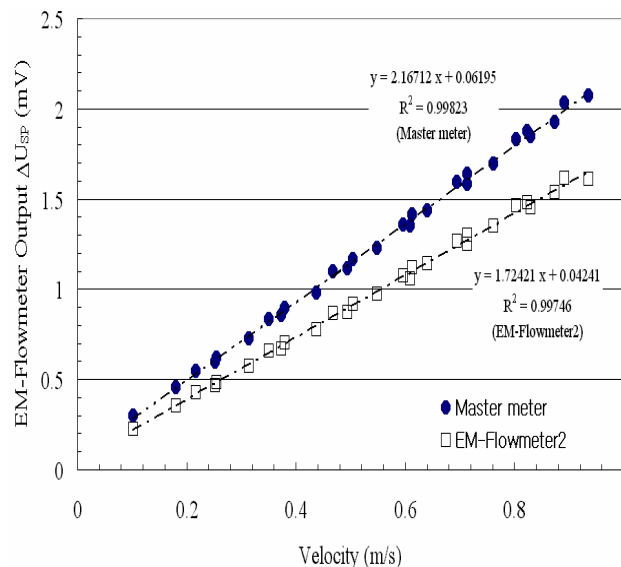


**Figure 8. Single-phase calibration data of electromagnetic flowmeter as a master-meter in LM loop**

Figure 10 shows the normalized output of flowmeter using the superficial liquid velocity  $j_f$  with void fraction. In fact, the void fraction was not measured directly with any device in this system. Thus the void fraction was calculated with two electromagnetic flowmeters with Equation (6) under the assumption of the ratio of correction factor ( $K_1/K_{f0}$ ) = 1.0. The normalized values are linearly varied in the low void fraction, which is similar inclination to

water-air two-phase experiments. However, this does not mean the actual value since the correction factor is a function of fluid conductivity, which must be determined or coupled by void fraction.

Figure 11 was obtained with iteration method using the Equation (7), Equation (8), and the conductivity by Petrick<sup>(12)</sup>. The nomalized values are changed with along the dotted line in Figure 10. This means that the void fraction can be simply measured with two electromagnetic flowmeters for a low-void fraction flow such as bubbly flow with some error margins.

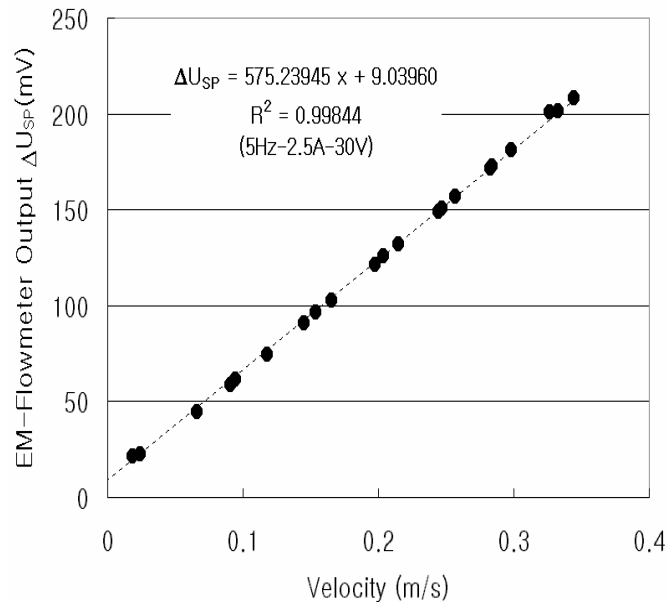


**Figure 9. Single-phase calibration data of AC electromagnetic flowmeter in LM loop**

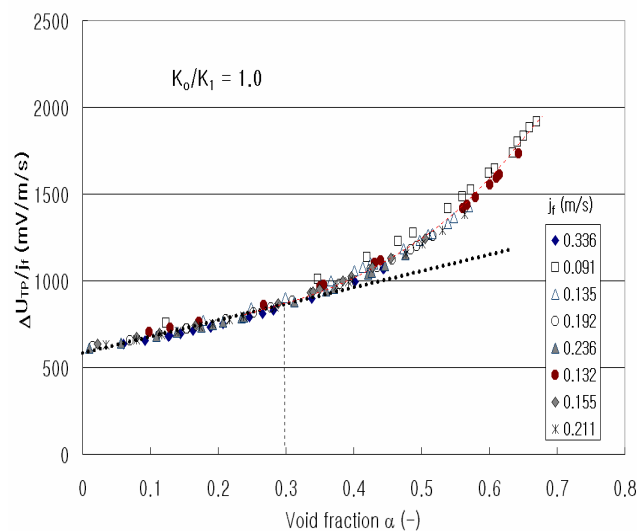


**Figure 10. Normalized output of electromagnetic flowmeter with void fraction (sodium-nitrogen)**

Thus, the flowmeters can be used to measure the void fraction for a liquid sodium within some tolerable error margins. Figure 12 shows the raw signal of electromagnetic flowmeter in the region of bubbly flow. The flow signal in bubbly flow is the same as the single phase flow. This pattern is very similar to water-air experiments.

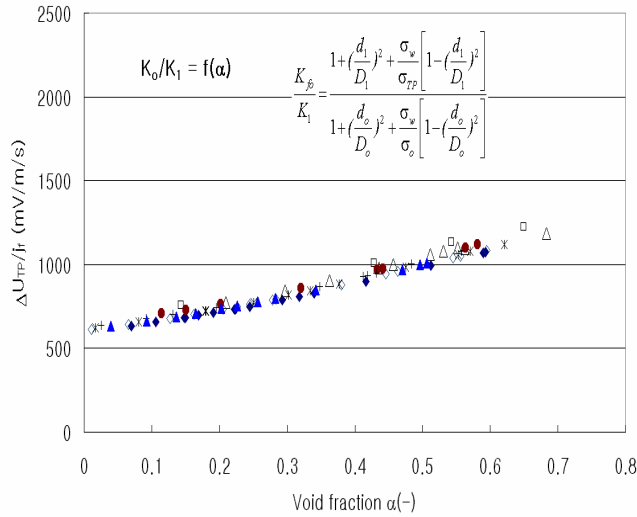


**Figure 11. Normalized output of electromagnetic flowmeter with void fraction calculated by the correction factor**

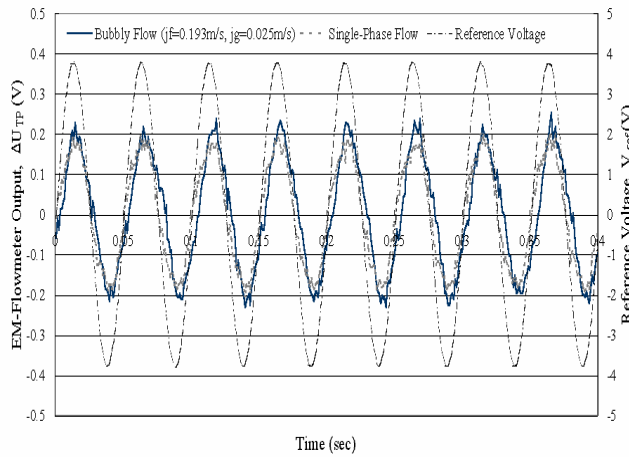


**Figure 12. Raw signal of electromagnetic flowmeter in the bubbly flow (sodium-nitrogen)**

## 5. Conclusions

A series of experiments were conducted to study the characteristics of the electromagnetic flowmeter in the liquid metal two-phase flow. For this study, AC electromagnetic flowmeters were designed and manufactured. Before the liquid metal experiments, the various signals

including noise were obtained from the flowmeter in the water-air two-phase flow and analyzed in connection with the images of the flow pattern captured by the high-speed CCD camera. The two-phase measurements were conducted in the liquid metal loop to confirm the feasibility obtained from water-air experiments as a measuring device for the two-phase flow.

The major conclusions of the present work can be encapsulated as followings:

- 1) The AC electromagnetic flowmeters were designed and manufactured, and showed excellent performance in both single-phase and two-phase bubbly flow. For two-phase bubbly flow, the liquid flow rate in a liquid-gas mixture can be measured directly only if a void fraction  $\alpha$  is estimated both in water-air and sodium-nitrogen two-phase flow.
- 2) The instantaneous location of a slug bubble can be detected by the phase change of the raw signal that has the transformer emf as well as the motional emf. In addition, the instantaneous change of liquid velocity around the slug bubble can be measured.
- 3) For bubbly flow, the discrepancy between the experimental results and the simple relation  $\Delta U_{TP} = \Delta U_{SP} / (1 - \alpha)$  is found, and the deviation is slightly increased with void fraction  $\alpha$  and also superficial liquid velocity  $j_f$ . It can be concluded that the measurement accuracy is decreased when void fraction  $\alpha$  and also superficial liquid velocity  $j_f$  are large due to non-homogeneity in two-phase flow.
- 4) While there is no difference in the shape of the raw signal between single-phase and bubbly flow, the signal amplitude for bubbly flow is higher than that for single-phase flow at the same water flow rate. This is caused by the reduction in the area of the liquid-flow passage. The same phenomena can be obtained in the liquid-metal two-phase flow.
- 5) The void fraction can be simply measured with two electromagnetic flowmeters for a low-void fraction flow such as bubbly flow with some error margins. Thus, the flowmeters can be used as a void-fraction measurement device for a liquid sodium within some tolerable error margins.

### Acknowledgement

This work was carried out with the support of the National Laboratory of Two-phase Flow and Phase Change Heat Transfer supported by MOST, Korea. The authors are grateful for their support.

### Nomenclature

- $A$  = cross-sectional area of flowtube [ $\text{mm}^2$ ]
- $b$  = inner radius of tube wall in the flowtube [mm]
- $B, B$  = magnetic flux density [Gauss]
- $D$  = outer diameter of flowtube [mm]
- $d$  = inner diameter of flowtube [mm]
- $I$  = current input into the magnet coil [A]
- $\mathbf{j}$  = virtual current density [ $\text{A}/\text{m}^2$ ]
- $j$  = superficial fluid velocity [m/s]

$\dot{m}$  = mass flow rate of fluid [kg/s]  
 $Q$  = volume flow rate [lpm, m<sup>3</sup>/s]  
 $\Delta P$  = total pressure drop ( $\Delta P = \Delta P_h + \Delta P_{tp} + \Delta P_{ac}$ ) [Pa]  
 $\Delta P_h$  = hydrostatic pressure drop [Pa]  
 $\Delta P_{tp}$  = two-phase frictional pressure drop [Pa]  
 $\Delta P_{ac}$  = accelerational pressure drop [Pa]  
 $U$  = electric potential [V]  
 $\Delta U_{AB}$  = potential difference between electrodes [V]  
 $\mathbf{v}$  = velocity vector [m/s]  
 $v$  = velocity [m/s]  
 $v_m$  = mean velocity [m/s]  
 $V_l$  = leakage voltage [V]  
 $V_m$  = flow induced voltage [V]  
 $V_{ex}$  = line input [V]  
 $V_{ref}$  = reference voltage [V]  
 $\mathbf{W}, W$  = weight vector, weight function  
 $\Delta z$  = hydraulic head [m]

### Greek Letters

$\alpha$  void fraction  
 $\sigma$  electrical conductivity [mho/m]  
 $\rho$  density [kg/m<sup>3</sup>]  
 $\tau$  integral volume

### Subscripts

$I$  test-position  
 $f$  liquid phase  
 $g$  gas phase  
 $L, l$  liquid phase  
 $o$  inlet position before injection of gaseous phase  
 $SP$  single-phase  
 $TP$  two-phase  
 $w$  wall

### References

- (1) Shercliff, J.A., (1954), "Relation between the velocity profile and the sensitivity of electromagnetic flowmeters," *J. Applied Physics*, **25**, 817-818.  
 Shercliff, J.A., (1962), *The theory of electromagnetic flow-measurement*, Cambridge University Press.
- (2) Elrod, H.G. and Fouse, R.R., (1952), "An investigation of electromagnetic flowmeters,"

*Transactions of The ASME*, 589-593.

(3) Bernier, R.N. and Brennen, C.E., (1983), "Use of the electromagnetic flowmeter in a two-phase flow," *Int. J. Multiphase Flow*, **9**(3), 251-257.

(4) Wyatt, D.G., (1986), "Electromagnetic flowmeter sensitivity with two-phase flow," *Int. J. Multiphase Flow*, **12**(6), 1009-1017.

(5) Hori, M., Kobori, T. and Ouchi, Y., (1966), *Method for measuring void fraction by electromagnetic flowmeters*, Nippon Genshiryoku Kenkyuho (Rep.), JAERI, No. 1111.

(6) Ochiai, M., Kuroyanagi, T., Kobayashi, K., and Furukawa, K., (1971), "Void fraction and heat transfer coefficient of sodium-argon two-phase flow in vertical channel," *J. Atomic Energy Society of Japan*, **13**, 566-573.

(7) Murakami, M., Maruo, K. and Yoshiki, T., (1990), "Development of an electromagnetic flowmeter for studying gas-liquid, two-phase flow," *International Chemical Engineering*, **30**(4), 699-702.

(8) Velt, I.D., Petrushaitis, V.I., Sprjgin, B.S., Krasilnikov, I.V., Mikhailov, Yu.V. and Tuleninov, V.R., (1982), "Correlation technique for flow rate measurement of electroconductive fluids and two-phase media and device for its implementation.," (Patent No. 30.01.82)

(9) Krafft, R., (1993), *Electromagnetic flowmeters in multiphase flows*, Ph.D. Thesis, Cranfield Inst. of Technology.

(10) Heineman, J.B., Marchaterre, J.F., and Mehta, S., (1963), "Electromagnetic flowmeters for void fraction measurement in two-phase metal flow," *The Rev. of Scientific Instruments*, **34**(4), 399-401.

(11) Bevir, M. K., (1970), "The theory of induced voltage electromagnetic flowmeters," *J. Fluid Mechanics*, **43**, part 3, 577-590.

(12) Pretrick, M. and Lee, K.Y., (1964), *Performance characteristics of a liquid metal generator*, Argonne National Lab., ANL-6870.

(13) Watanabe, M., (1977), "Noise compensation in electromagnetic flowmeter," US Patent 4,019,385.

(14) Cha, J.E., Ahn, Y.C., and Kim, M.H., (2002), "Flow measurement with an electromagnetic flowmeter in two-phase bubbly and slug flow regimes," *Flow Measurement and Instrumentation*, Vol.12, 329-339.

(15) Lockhart R.W. and Martinelli R.C., (1949), "Proposed correlation of data for isothermal two-phase, two-component flow in pipes," *Chemical Engineering Progress*, **45**(1), 39-48.

(16) Georges E. S., (1963), *Two-component two-phase flow parameters for low circulation rates*, Argonne National Lab., ANL-6755.

(17) Mishima, K. and Ishii, M., (1984), "Flow regime transition criteria for upward two-phase flow in vertical tubes," *Int. J. Heat Mass Transfer*, **27**(5), 723-737.